

High-Precision Timing of 5 Millisecond Pulsars: Space Velocities, Binary Evolution and Equivalence Principles

M. E. Gonzalez¹, I. H. Stairs¹, R. D. Ferdman², P. C. C. Freire³, D. J. Nice⁴, P. B. Demorest⁵, S. M. Ransom⁵, M. Kramer³, F. Camilo⁶, G. Hobbs⁷, R. N. Manchester⁷, A. G. Lyne²

ABSTRACT

We present high-precision timing of five millisecond pulsars (MSPs) carried out for more than seven years; four pulsars are in binary systems and one is isolated. We are able to measure the pulsars' proper motions and derive an estimate for their space velocities. The measured two-dimensional velocities are in the range 70–210 km s⁻¹, consistent with those measured for other MSPs. We also use all the available proper motion information for isolated and binary MSPs to update the known velocity distribution for these populations. As found by earlier works, we find that the velocity distribution of binary and isolated MSPs are indistinguishable with the current data. Four of the pulsars in our observing program are highly recycled with low-mass white dwarf companions and we are able to derive accurate binary parameters for these systems. For three of these binary systems we are able to place initial constraints on the pulsar masses with best-fit values in the range 1.0–1.6 M_⊙. The implications of the results presented here to our understanding of binary pulsar evolution are discussed. The updated parameters for the binary systems studied here, together with recently discovered similar systems, allowed us to update previous limits on the the violation of the strong equivalence principle through the parameter $|\Delta|$ to 4.6×10^{-3} (95% confidence) and the violation of Lorentz-invariance/momentum-conservation through the parameter $|\hat{a}_3|$ to 5.5×10^{-20} (95% confidence).

Subject headings: binaries: close — stars: neutron — stars: pulsar — relativity

1. Introduction

Pulsars are believed to be born with spin periods of ~ 0.1 s and gradually slow down as they

age due to the loss of rotational kinetic energy in the form of electromagnetic radiation. These “normal” pulsars make up the bulk of the observed population and $\sim 1,900$ of them are currently known (Manchester et al. 2005)¹. On the other hand, a group of old, fast-spinning pulsars is observed (~ 200 pulsars). It is believed that these old pulsars are formed from the transfer of mass and angular momentum from a previous or present companion in a binary system (Alpar et al. 1982). These pulsars are generally seen as “recycled” members of the population: old pulsars that have been spun-up and brought back to an active, pulse-emitting life thanks to their interaction within a binary system. The fastest spin-

¹Department of Physics and Astronomy, University of British Columbia, 6224 Agricultural Road, Vancouver, BC, V6T 1Z1, Canada; gonzalez@phas.ubc.ca1

²Jodrell Bank Centre for Astrophysics, University of Manchester, Manchester, M13 9PL, UK

³Max-Planck-Institut für Radioastronomie, Auf dem Hügel 69, D-53121 Bonn, Germany

⁴Physics Department, Lafayette College, Easton, PA 18042, USA

⁵National Radio Astronomy Observatory, Charlottesville, VA 22903, USA

⁶Columbia Astrophysics Laboratory, Columbia University, New York, NY 10027, USA

⁷Australia Telescope National Facility, CSIRO, Epping NSW 1710, Australia

¹See also the ATNF Pulsar Catalogue: <http://www.atnf.csiro.au/research/pulsar/psrcat/>.

ning pulsars known have spin periods of $P_s \lesssim 0.01$ s, so-called “millisecond pulsars” (MSPs), and are thought to have been produced in this manner. The measured characteristics of the members of these binary systems and their orbital parameters provide valuable insights into the formation and evolution of these systems. See, e.g., Stairs (2004) and Lorimer (2008) for general reviews of binary pulsars and their scientific importance.

The measurement of a pulsar’s proper motion can be used to estimate its space velocity (e.g., Hobbs et al. 2005; Chatterjee et al. 2009). Such measurements are important for a variety of scientific questions, including estimating the distribution of natal kicks imparted to proto-neutron stars by the supernova (SN) explosion that created them. A variety of mechanisms have been proposed that can give rise to these natal kicks (e.g., Spruit & Phinney 1998; Kusenko & Segrè 1999; Jessner et al. 2005). Another key question is whether isolated MSPs have a similar velocity distribution to those still in binary systems (e.g., Tauris & Bailes 1996; Toscano et al. 1999; Lommen et al. 2006; Hobbs et al. 2005; McLaughlin et al. 2005). In general, we expect MSPs to have lower system velocities than the rest of the pulsar population since, after the SN explosion, the binary system must have remained intact to spin up the neutron star. However, for isolated MSPs, the companion must eventually leave the system or be evaporated. Arguments for both lower and higher velocities for isolated MSPs have been given in the literature (e.g., Toscano et al. 1999; McLaughlin et al. 2005). Given that only a small number of isolated MSPs with measured proper motions are known (<10 objects), additional measurements are very important.

Many subclasses of pulsar binary systems are now recognized (e.g., Stairs 2004; Lorimer 2008). The broader distinction made is between those pulsars with high-mass companions (e.g., another neutron star) and those with lower mass companions (e.g., white dwarfs – WDs). In the case of pulsars with WD companions, various subgroups are generally identified. For example, mildly-recycled pulsars ($P_s \sim$ tens of milliseconds) in a tight orbit (orbital periods $P_b \lesssim$ a few days) with high-mass WD companions ($m_2 \sim 1 M_\odot$) are thought to arise from a common-envelope evolution or from periods of ultra-high mass transfer during a

Roche-lobe overflow phase (van den Heuvel 1994; Tauris et al. 2000).

A more straightforward evolution is thought to apply for MSPs in long orbits ($P_b \gtrsim 4$ days) with low-mass WD companions ($m_2 \lesssim 0.3 M_\odot$), generally called wide-orbit binary millisecond pulsars (WBMSp; Rappaport et al. 1995; Tauris & Savonije 1999). Here, as the companion evolves and overflows its Roche-lobe during the red-giant phase, mass spirals onto the neutron star and forms an accretion disk. A stable, long-lived mass transfer phase is expected to take place, producing nearly circular orbits (eccentricities of $e \sim 10^{-6}$ – 10^{-3}). Phinney (1992) predicted that these systems should exhibit an orbital period–eccentricity ($P_b - e$) relationship based on the expectation that convective eddies in the envelope of the red giant will produce nonzero values of the eccentricity. The point at which mass transfer ceases and e freezes depends on the size of the red giant envelope, which will in turn determine the size of the orbit and thus the orbital period. In addition, the size of the envelope is also thought to be related to the mass of the red giant’s core, which eventually contracts to form a WD. Therefore, an orbital period–core mass ($P_b - m_2$) relationship is also expected in these systems (Rappaport et al. 1995; Tauris & Savonije 1999).

The WBMSp systems also provide important tests for theories of gravity. For example, the strong equivalence principle (SEP) states that all neutral test masses fall with the same acceleration in an external gravitation field, i.e., it states that the gravitational and inertial masses of self-gravitating bodies are identical ($m_g/m_i \equiv 1$). Binary pulsar systems allow us to test for SEP violations in the limit of high self-gravity (Damour & Schäfer 1991; Wex 1997, 2000; Stairs et al. 2005): if the binary components experience different accelerations in the gravitational field of the Galaxy, a forced eccentricity is imparted to the system along the projected direction of the external force onto the orbital plane. Binary pulsars with low companion mass, small eccentricity and long orbital periods are ideal for SEP violation tests.

Another important test of gravitational theories involves the post-Newtonian parameter α_3 which is associated with the violation of momentum conservation and the existence of preferred frames

(Lorentz invariance; Will 1993). In general relativity (GR), $\alpha_3 \equiv 0$. The most observable effect of a possible deviation from this GR prediction is thought to be a non-zero self-acceleration for a rotating body in a direction perpendicular to its spin axis and perpendicular to its velocity with respect to the absolute rest frame (Bell & Damour 1996). In the case of binary systems, each component will experience self-acceleration. These self-accelerations perturb the orbital dynamics, leading to a forced eccentricity and polarization of the orbit along a fixed direction.

Here we present results obtained from long-term timing of 5 MSPs, four of which are WBMSPs (PSR J1853+1303, PSR J1910+1256, PSR B1953+29, PSR J2016+1948) and one of which is isolated (PSR J1905+0400). We use our results to study the space velocities of MSPs, binary evolution models and equivalence principle tests. In §2 we describe the observations performed and data analysis carried out. In §3 we present our improved timing solution for these pulsars, including the measured proper motions. In §3.1 we discuss the implications for the velocity distribution of isolated and binary MSPs and discuss their implications for binary evolution models of MSPs. In §3.2 we derive constraints on the component masses for three systems and we discuss these results in light of evolution models. In §3.3 we present updated upper limits of equivalence principle violations using WBMSPs. Finally, in §4 we summarize our findings and point to future directions of this research.

2. Observations and Data Analysis

We have conducted high-precision timing on four WBMSPs and one isolated MSP. We collected data from two observatories and a total of five data acquisition systems. Here we describe the observing setups used at each telescope. A summary of the observations for each pulsar is given in Table 1.

2.1. Arecibo

All pulsars were observed with the 305-m Arecibo telescope in Puerto Rico. The Wideband Arecibo Pulsar Processors (WAPPs; Dowd et al. 2000) were used to observe all the pulsars. Three of the four WAPPs were used for most pulsars, ex-

cept PSR J2016+1948 for which all four WAPPs were used in some observations. They were operated in online folding mode with 32 μs sampling and 192 lags near 1400 MHz and 96 lags at 2700 MHz (for PSR J2016+1948 a sampling time of 128 μs and 128 lags were used). The Arecibo Signal Processor (ASP; Demorest 2007) was used for all pulsars except PSR J2016+1948. ASP provides 0.25 μs complex sampling in two orthogonal polarizations. These data were coherently de-dispersed in software using 16 or 24 frequency channels, each with 4 MHz bandwidth. The polarisations were later summed and the signal folded at the pulsar period. The ASP observations were flux calibrated with a pulsed noise diode of known strength and, when available, with observations of a standard flux calibration source. A typical observing session involved collecting multiple integrations of 1 or 3 min long on each pulsar with ASP and the WAPPs for a total of up to 30 min of data. The data from the short integrations were aligned and summed using a preliminary timing model. For the WAPPs, all data were summed to obtain a single profile for each observation. For ASP, a separate profile was obtained at each frequency channel for each observation.

For PSR J2016+1948 we also used data from the Penn State Pulsar Machine (PSPM; Cadwell 1997), an analogue filterbank with 128×60 kHz frequency channels. The power level for each 128 channels was sampled every 80 μs and stored to tape. The data were subsequently folded and aligned multiple times as the ephemeris for the pulsar was being refined. The PSPM and WAPP data for this pulsar were summed every few minutes and multiple profiles were obtained for most epochs.

To provide a long time baseline and improve the measured proper motion for PSR B1953+29 we also used data taken with the Mark II system (Rawley 1986), a dual-polarization 32×30 kHz filterbank spectrometer. Here, the outputs from opposite polarizations were summed and sampled at the pulsar period. Data were averaged over intervals of 1-2 minutes and stored for off-line processing. A total of around 1 hour of data were collected at each epoch and the data summed to obtain one profile for each observation².

²Additional data for PSR B1953+29 from Arecibo (MJD

2.2. Parkes

We used the 64-m Parkes telescope in NSW, Australia to observe pulsars PSR J1853+1303, PSR J1905+0400 and PSR J1910+1256. These observations were taken using the Parkes analogue filterbank centered at 1390 MHz with 512×0.5 -MHz frequency channels sampled every 0.25 ms. Two polarizations were recorded and summed in hardware for each frequency channel. The data were subsequently folded off-line using a preliminary ephemeris and summed to obtain a single profile for each observation.

A time of arrival (TOA) was found for each observation by cross-correlating the profiles with a high signal-to-noise standard template (Taylor 1992). The recorded observatory times were corrected to UTC time by using data from GPS satellites. The JPL DE405 ephemeris (Standish 2004) was used for barycentric corrections. The software package TEMPO³ was used to find the timing solution for each pulsar by including astrometric, binary and spin parameters as needed to arrive at a phase-connected solution (where every rotation of the star over the span of the observations is accounted for). In order to fit for any instrumental or standard template profile differences, we fit for arbitrary time offsets between each instrument (for ASP we have also allowed for time offsets between each 4 MHz channel to fit for any profile changes across its bandwidth). A change in dispersion measure (DM) over time was detected for PSR J2016+1948 and marginally for PSR J1905+0400 and PSR B1953+29 (see Table 2). Finally, the measured uncertainties were scaled by a small telescope-dependent amount to ensure a timing fit with $\chi^2_{\nu} \simeq 1$.

3. Results and Discussion

In Figure 1 we show the standard pulse profiles for each pulsar at 1400 MHz. Table 2 shows the timing solutions derived from our work and Figure 2 shows the timing residuals derived from these solutions. The timing solutions successfully

model the measured TOAs and leave no significant trends in the residuals. Pulsars PSR J1853+1303 and PSR J1910+1256 have very low root-mean-square (rms) values and are now part of a long-term timing program to detect and study gravitational waves using an array of well-timed pulsars (Hobbs et al. 2010; Demorest et al. 2009, 2011).

PSR J1853+1303 and PSR J1910+1256 were discovered by the Parkes multibeam pulsar survey (e.g., Manchester et al. 2001) and their timing solutions were first reported by Stairs et al. (2005). The longer data span possible with the Parkes data and the high quality of the Arecibo data allowed us to improve the timing solutions for these pulsars (especially for their binary parameters) and, for the first time, report a measurement of their proper motions. For PSR J1910+1256, we are also able to measure a secular change in its projected semimajor axis (a similar, though marginal, measurement was also made for PSR J1853+1303).

PSR B1953+29 was discovered while performing a systematic search for radio pulsars using Arecibo in position error boxes from γ -ray sources reported by the COS B satellite (Boriakoff et al. 1983). Previous timing solutions for PSR B1953+29 have been reported by Rawley et al. (1988) and Wolszczan et al. (2000). Here we have been able to use Arecibo data spanning 25 yrs to derive a much improved timing solution for this pulsar, and especially so for its proper motion measurement. PSR J1905+0400 was also discovered by the Parkes multibeam pulsar survey (Hobbs et al. 2004) and is one of only <20 known isolated MSPs. Here we are able to measure for the first time a proper motion for this pulsar.

PSR J2016+1948 was discovered in the Arecibo 430 MHz Intermediate Latitude Survey (Navarro et al. 2003). The discovery dataset for this pulsar covered about a year (taken in 1999) and were enough to determine that the pulsar was in a binary system with an unusually long orbital period of 635 days. However, deriving a complete timing solution from this initial dataset was not possible. It was later discovered that the original 1999 data have large systematics, most likely the result of being folded with an inaccurate estimate for the spin period. These data have been left out of our analysis and all subsequent data were

49129–49255) and the Effelsberg telescope in Germany (MJD 49768–50460) were also available but did not add significantly to the results and were left out of our analysis.

³<http://tempo.sourceforge.net/>.

taken in observing modes that allow for re-folding and re-aligning as the pulsar ephemeris was being improved. The current timing solution leaves no systematics in the derived TOAs and has been correctly predicting new TOAs for many years. We are therefore confident that we have found the most precise timing solution currently available for this system. Our timing solution in Table 2 shows that the pulsar is indeed recycled and in a nearly circular orbit, likely the result of mass transfer and tides as its companion was going through its giant phase. We are also able to measure the proper motion for this system and a secular change in the projected semimajor axis.

None of the pulsars show a significant value of annual parallax (see Table 2). Only PSR J1853+1303 has a marginal parallax measurement with a large error. It is possible that further observations of this pulsar with improved timing precision will be able to produce a more constraining parallax measurement. In addition, none of the binary pulsars show a measurable Shapiro delay. The residuals obtained from the best-fit timing solution are shown as a function of binary phase in Figure 3.

3.1. Millisecond Pulsar Velocities

The high precision obtained by our timing study allowed us to measure a statistically significant value for the proper motions of all five pulsars (see Table 2). We have used these measurements to study the velocity distribution of MSPs, both isolated and those in binary systems. The pulsar population in general has been found to have large space velocities with a mean of $\sim 300 \text{ km s}^{-1}$ (Lyne & Lorimer 1994; Hobbs et al. 2005). Recycled MSPs appear to be on the low end of the velocity distribution, with a mean of $\sim 90 \text{ km s}^{-1}$. In addition, no significant difference has been found between the velocities distributions of isolated MSPs and those still in binary systems (Hobbs et al. 2005; Lommen et al. 2006) despite the fact that an additional evolutionary stage (the disruption of the binary) has occurred in the former.

Now we revisit the velocity distribution of MSPs, which we take to be those with periods of $P < 0.01$ sec and are therefore fully recycled. From the new timing solutions presented in Table 2, only PSR J2016+1948 is not a fully recycled

MSP and its implied 2D velocity of 96 km s^{-1} (at the implied DM distance of 2.5 kpc) was not included in the following analysis. PSR J1905+0400 studied here is particularly important, as it is one of only ten isolated MSPs with measured proper motions. Our sample then consists of 10 isolated MSPs and 27 binary MSPs for a total of 37 pulsars. We have combined the measured proper motions with the available distance estimates to calculate the pulsars' 2D space velocities in their respective local standard of rest at the pulsar location. To do this we have corrected for Solar motion and used a peculiar velocity for the Sun of $V_{\odot} = 13.4 \text{ km s}^{-1}$ (Dehnen & Binney 1998). We have also assumed a flat Galactic rotation curve with a galactocentric distance for the Sun of $R_{\odot} = 8 \text{ kpc}$ and a Galactic rotation velocity of 222 km s^{-1} (Eisenhauer et al. 2003; Dehnen & Binney 1998). A flat Galactic rotation curve is thought to be a good approximation for distances from the Galactic centre of $>3 \text{ kpc}$ (Olling & Merrifield 1988; the pulsars we used have distances to the Galactic center of $>4 \text{ kpc}$). The resulting 2D velocities in the pulsars' standard of rest after correcting for Solar and Galactic motion, V_{2D} , are shown in Table 3.

Most pulsars have distance estimates from timing measurements of their dispersion measure (DM) combined with a model of the free electron distribution in the Galaxy (Cordes & Lazio 2002). In general, distances derived using this method are thought to have a $\sim 25\%$ error, implying a minimum similar error on the estimated velocities. For individual pulsars, the distance error could be much larger than that. The errors on the estimated pulsar velocities shown in Table 3 were derived using Monte Carlo simulations with 10,000 runs per pulsar. For these simulations, pulsar distances were drawn from Gaussian distributions centered on the values listed in Table 3 with a width of 25% of the central value⁴ (for pulsars where non-DM distances are available the corresponding distance errors were used). Pulsar proper motions were then drawn using Gaussian distributions with central values and widths derived using the values listed in Table 3. In practice, the largest error contribution to the esti-

⁴This uncertainty is consistent with the $\sim 20\%$ estimate of uncertainty in distances due to unmodeled inhomogeneities in the interstellar medium model (Cordes & Lazio 2003).

mated pulsar velocities are the associated distance errors. We then used the velocities in Table 3 to study the velocity distribution of MSPs.

Figure 4 shows the normalized histograms of the 2D velocities of binary (solid line) and isolated MSPs (bold dotted line) in our sample. The average velocities are found to be 108 ± 15 , 113 ± 17 and 93 ± 20 km s^{-1} for all MSPs, binary MSPs and isolated MSPs, respectively⁵. The average 2D velocities without correcting to the pulsars’ standard of rest are 88 ± 12 , 96 ± 15 and 68 ± 16 km s^{-1} for all, binary, and isolated MSPs, respectively. The updated velocities are consistent with previous work: Hobbs et al. (2005) reported 2D uncorrected velocities for binary and isolated MSPs of 89 ± 15 and 76 ± 16 km s^{-1} , respectively, with Lommen et al. (2006) and McLaughlin et al. (2005) reporting similar values. We then find that the average velocities of binary and isolated MSPs are consistent with each other. To test whether the two samples are consistent with arising from the same distribution we use the Kolmogorov-Smirnov (KS) test (Massey 1951)⁶. A KS test of the two corrected velocities results in a probability of 62% that they are drawn from the same distribution. For the uncorrected 2D velocity measurements, the two distributions have a KS probability of 75% that they are drawn from the same distribution.

We therefore conclude that there is no statistically significant difference between the velocity distributions of isolated and binary MSPs with the current statistics. However, we also note that due to selection effects our sample is biased towards nearby, low-velocity pulsars. It is therefore possible that the lack of difference between the velocity distribution of isolated and binary MSPs is due to our observing the low velocity tail of these distributions, which in reality could be quite different. Higher number statistics (particularly for isolated MSPs) will allow for a more detailed study of such effects in the future. In addition, more distant MSPs are now being discovered in current surveys

⁵The errors in the average velocities shown in this section represent the standard errors of the mean.

⁶While the KS test doesn’t take the error estimates into account, it is one of the most useful and general methods for comparing two samples. Detailed simulations to account for the errors are beyond the scope of this paper and can be carried out in future work.

(e.g., in addition to PSR J1903+0327 in Table 3, the velocities for two distant MSPs will also be published by Deneva et al. 2011). While measuring the proper motions of distant objects will most likely require large amounts of telescope time, they represent significant additions to our sample.

Furthermore, we note that Tauris & Bailes (1996) presented the expected space velocities of binary MSPs using various evolutionary models. In their simulations, binaries with shorter periods tend to have larger velocities since the final velocity of the system depends on the separation of the components at the time of the supernova explosion. However, this correlation is fairly weak and asymmetries in the explosion would easily wipe out this effect. Hobbs et al. (2005) found no evidence for a correlation between the velocity of binary MSPs and their binary periods⁷. We now briefly revisit this idea and in Figure 5 we plot the binary periods versus implied velocity for the binary pulsars listed in Table 3. This figure should be compared to the plots in Figure 2 of Tauris & Bailes (1996). For system with $P_b < 2$ days and $P_b > 2$ days we find average 2D velocities of 135 ± 52 km s^{-1} and 107 ± 14 km s^{-1} , respectively (uncorrected 2D velocities have averages of 120 ± 45 km s^{-1} and 85 ± 11 km s^{-1}).

We therefore find no significant difference in the velocities of short- and large-period binary MSPs. However, we caution that only a handful of the former systems are known. While the very large velocity of PSR B1957+20 could be explained by these models using asymmetries in the supernova explosion, they would have a particularly hard time explaining the small implied velocities for PSR J0751+1807 and PSR 2051–0827 given their very short orbital periods. In addition, we did simulations using the Tauris & Bailes (1996) binary period–velocity relationship taking into account the effect of random projections towards us of these velocities. We find that the large scatter in the relationship and the random projections of these velocities would most likely wash out any effect. Therefore, while we find no evidence that the relationship is present (and this might indeed

⁷Hobbs et al. (2005) used a definition of $P < 0.1$ s and $\dot{P} < 10^{-17}$ s s^{-1} for recycled pulsars, thus including a mix of companion types in their sample. Here we use $P < 0.01$ s, resulting in binaries with mostly helium white dwarf companions.

be very difficult to achieve, even if it exists), at the same time we cannot rule it out. It is clear that additional work is needed to understand the evolution of binary MSPs. Obtaining additional velocity measurements for these pulsars will help to constrain evolutionary models.

3.2. Component masses and change in projected semimajor axis

For PSR J1910+1256 and PSR J2016+1948 we were able to measure a change in the projected semimajor axis, $\dot{x}=dx/dt$ (see Table 2). For PSR J1853+1303, the measurement of \dot{x} was marginal and will be discussed at the end of this section. For PSR B1953+29 only an upper limit was measured. Here we define $x\equiv a_1\sin i/c$, where a_1 is the semi-major axis of the pulsar orbit, i is the inclination angle of the angular momentum vector of the orbit relative to the Earth-pulsar line of sight (LOS), and c is the speed of light. The measured values for \dot{x} are $-1.8(5)\times 10^{-14}$ and $8.3(14)\times 10^{-14}$ for PSR J1910+1256 and PSR J2016+1948, respectively. In principle, a non-zero value for \dot{x} could arise from a change in a_1 , i or a combination of the two. However, we argue that the measured values likely arise due to the pulsars' high proper motion inducing a change in our LOS to these binaries.

In the case that a change in a_1 is being observed, GR predicts a value of $|\dot{a}_1| \sim 5\times 10^{-23}$ and $\sim 10^{-24}$ for PSR J1910+1256 and PSR J2016+1948, respectively (see Peters 1964, for the required expression). These values are many orders of magnitude below the observed value of \dot{x} . In addition, for typical binary astrophysical processes, a non-zero value for $|\dot{a}_1/a|$ is expected to have a similar order of magnitude as $|\dot{P}_b/P_b|$. No significant value for \dot{P}_b was found for any of our pulsars, but allowing for a measurement in our timing solution results in a value of $\dot{P}_b=-2(4)\times 10^{-11}$ and $-1(2)\times 10^{-9}$ s s⁻¹ for PSR J1910+1256 and PSR J2016+1948, respectively. Using the values for P_b listed in Table 2 we find limits of $|\dot{P}_b/P_b| < 1.2\times 10^{-17}$ s⁻¹ and $< 5\times 10^{-17}$ s⁻¹ for PSR J1910+1256 and PSR J2016+1948, respectively. Again, these values are a few orders of magnitude lower than expected from the measured values of \dot{x} .

We therefore propose that the observed values of \dot{x} must arise from apparent changes in the orbital parameters due to the proper motion of

the binaries (Arzoumanian et al. 1996; Kopeikin 1996). The strength of this geometric effect can be calculated using:

$$\dot{x} = 1.54 \times 10^{-16} x \mu \cot i \sin \theta \text{ s s}^{-1} \quad (1)$$

where x is the projected semimajor axis in units of seconds, μ is the total proper motion of the system in units of mas/yr and θ is the unknown angle between the position angle of the proper motion and the position angle of the ascending node of the pulsar's orbit. The measured values of \dot{x} can then be used to constrain the inclination angle of the system i . Following Nice et al. (2001), we have used a Monte Carlo simulation to constrain the values of i that satisfy Equation 1 for both PSR J1910+1256 and PSR J2016+1948, resulting in 1σ values of $44^\circ(36^\circ-52^\circ)$ and $36^\circ(27^\circ-45^\circ)$, respectively.

In addition, numerical studies of the evolution of neutron star binaries in long-period orbits with low-mass white dwarf companions point to a relationship between the final orbital period, P_b , and the mass of the companion, m_2 (Rappaport et al. 1995; Tauris & Savonije 1999). An overall agreement with these results has been found in the available data, although these relationships appear to overestimate m_2 for systems with long periods and provide conflicting results for systems with short periods (Stairs et al. 2005).

Keeping these caveats in mind, we used the $P_b - m_2$ relationship found by Tauris & Savonije (1999), together with the inclination angle constraints from \dot{x} , to provide constraints on the masses of the PSR J1910+1256 and PSR J2016+1948 systems. The derived constraints on the companion masses are $m_2 = 0.30-0.34 M_\odot$ and $0.43-0.47 M_\odot$ for PSR J1910+1256 and PSR J2016+1948, respectively. These values and those implied by the mass functions are shown in Figure 6. Restricting m_2 to lie in the values implied by the $P_b - m_2$ relationship and using the inclination angles from \dot{x} we find 1σ values for the pulsar masses of $m_1 = 1.6\pm 0.6 M_\odot$ and $1.0\pm 0.5 M_\odot$ for PSR J1910+1256 and PSR J2016+1948, respectively.

For PSR J1853+1303, the measured value of \dot{x} is marginal (see Table 2) but can still be used to derive initial constraints on the system masses. Following the same procedure as outlined above results in a 1σ confidence interval for the incli-

nation angle of this system of $48^\circ(33^\circ\text{--}58^\circ)$. In addition, the $P_b - m_2$ relationship produces companion masses of $m_2 = 0.33\text{--}0.37 M_\odot$. Combining these results, we derive 1σ values for the mass of PSR J1853+1303 of $m_1 = 1.4\pm 0.7 M_\odot$.

The derived m_1 values are not very constraining, though fully within the expected mass ranges for neutron stars. Given that PSR J2016+1948 is only one of three WBMSPs with $P_b > 200$ days (see Table 4), further constraining the masses of this system by independent measurements and continued timing can provide a valuable constrain to binary pulsar evolution models.

3.3. Theories of Gravity: Tests

We have used the improved timing parameters for the four WBMSPs studied here, in addition to recently discovered systems, to update important tests of GR and other theories of gravity. In particular, we have modeled the forced eccentricity that would be imparted on the binary systems due to violations of the strong equivalence principle (SEP) using the parameter Δ , and the forced eccentricity that would be imparted due to violations of Lorentz invariance/momentum conservation using the parameter $\hat{\alpha}_3$. In GR, both parameters are predicted to be identically zero and $\hat{\alpha}_3$ is also predicted to be zero in most other theories of gravity.

For the SEP test parameter Δ , the additional, forced eccentricity imparted on the binary orbit is expected to be of the form (Damour & Schäfer 1991):

$$|\mathbf{e}_{F,\Delta}| = \Delta \frac{|\mathbf{g}_\perp| c^2}{2FGM(2\pi/P_b)^2} \quad (2)$$

where c is the speed of light, F is unity in GR and a function of m_1 and m_2 in alternate theories, G is Newton’s constant in GR, $M=m_1+m_2$, P_b is the binary period and $|\mathbf{g}_\perp|$ is the projection of the Galactic acceleration vector onto the orbital plane at the location of the pulsar. Here, the total observed eccentricity is then predicted to be $\mathbf{e}_{obs} = \mathbf{e}_N + \mathbf{e}_{F,\Delta}$, with the “natural” eccentricity \mathbf{e}_N and the angle θ between \mathbf{e}_N and $\mathbf{e}_{F,\Delta}$ being additional, unknown parameters.

For the Lorentz invariance/momentum conservation test parameter $\hat{\alpha}_3$, the forced eccentricity added to the binary orbit is expected to be given

by (Bell & Damour 1996):

$$|\mathbf{e}_{F,\hat{\alpha}_3}| = \hat{\alpha}_3 \frac{c_P |\mathbf{V}| P_b^2}{24\pi P} \frac{c^2}{GM} \sin \beta \quad (3)$$

where $c_P = -2E_P^{grav}/m_1 c^2$ is the gravitation self-energy fraction of the pulsar (the so-called “compactness”, taken to be approximately $0.21m_1$; Damour & Esposito-Farèse 1992; Bell & Damour 1996), β is the unknown angle between the pulsar system’s absolute velocity \mathbf{V} (with respect to the reference frame of the cosmic microwave background) and the pulsar’s spin vector.

We have used the above expressions and a Bayesian analysis to derive probability distributions for Δ and $\hat{\alpha}_3$ given the measured binary/pulsar parameters and additional estimates for the remaining unknown parameters. The procedure was described in detail in Stairs et al. (2005) and we summarize it here⁸. For each pulsar j , we find the probability density functions (pdf) $p(|\Delta| | D_j, I)$ and $p(\hat{\alpha}_3 | D_j, I)$ for probable values of Δ and $\hat{\alpha}_3$ given each pulsar’s data D_j (see Table 4) and prior relevant information I .

For example, for the SEP parameter Δ we can write for each pulsar:

$$p(|\Delta|, d_j | D_j, I) \propto p(D_j | |\Delta|, d_j, I) \times p(|\Delta|, d_j | I) \quad (4)$$

where d_j represents the relevant parameters for this test, namely i , m_2 , Ω , d , e_N , and θ . For these parameters we perform Monte Carlo simulations when they are not directly measured or constrained through timing or other methods. For m_2 we use twice the range given by the $P_b - m_2$ relationship of Tauris & Savonije (1999). For $\cos i$ we assume a uniform distribution between 0 and 1, and combine this value with the measure mass function and m_2 to provide a value for the pulsar mass m_1 (only systems with m_1 values between 1.0 and 2.5 are kept)⁹. For Ω we use a uniform distribution between 0° and 360° . For d we use a Gaussian centered on the DM estimate using Cordes & Lazio (2002) and assuming an average uncertainty of 25%, or a Gaussian centered on the parallax measurement if available. The integrals

⁸We have also fixed some small bugs in the Stairs et al. (2005) code that did not significantly affect their results.

⁹For the pulsars presented here with new measured values for \dot{x} , we have not included the implied orbital constraints as they have large error bars.

over the remaining unknown parameters e_N and θ are computed separately using the measured values of \mathbf{e}_{obs} and ω and the implied values of $\mathbf{e}_{F,\Delta}$. A pdf for the $\hat{\alpha}_3$ parameter was similarly derived; for this we also need estimates for the 3D velocity of each pulsar and used Gaussian distributions in each dimension centered on the Galactic rotational velocity vector at the pulsar location with widths of 80 km s^{-1} (Lyne et al. 1998) or, when available, we use Gaussian distributions for the proper motions to get the transverse velocities. For $|\Delta|$, the parameter space $10^{-5} < |\Delta| < 0.1$ was sampled uniformly in steps of 2×10^{-5} and for $|\hat{\alpha}_3|$ the parameter space $10^{-22} < |\hat{\alpha}_3| < 5 \times 10^{-19}$ was sampled uniformly in steps of 1×10^{-22} .

Binary systems suitable for these studies are required to have large periods and small eccentricities so that additional relativistic effects are negligible. Large values of P_b^2/e and P_b^2/Pe have therefore been used as a general selection characteristic for choosing appropriate systems (Wex 2000; Stairs et al. 2005). In addition, the systems must be old enough and have large enough $\dot{\omega}$ so that the orientation of their orbits can be assumed to be random and that the projection of the Galactic acceleration vector on the orbit can be assumed to have been constant over the lifetime of the systems (Damour & Schäfer 1991; Wex 1997). While some pulsars might individually provide low limits for these tests, we use all 27 available systems in order to provide a more conservative upper limit that incorporates the assumptions made on the population as a whole.

Currently, a total of 27 WBMSPs are available to test the above effects and their properties are listed in Table 4. The pdfs for each pulsar are shown in Figure 7 for the SEP parameter $|\Delta|$ and in Figure 8 for the Lorentz invariance/momentum conservation parameter $|\hat{\alpha}_3|$. Since each pulsar represents an independent test of these parameters, we can multiply the individual pdfs to obtain a total pdf from our sample of pulsars.

Using all the systems in Table 4, for $|\Delta|$ we derive a 95% upper limit of 4.6×10^{-3} , which represents a 20% improvement from the value derived by Stairs et al. (2005). Two new pulsars are particularly constraining for this test: PSR J1711–4322 and PSR J1933–6211, which together with the improved parameters for PSR J1853+1303 have significantly contributed to the

reduced upper limit for $|\Delta|$ (the secondary peak at low values of $|\Delta|$ of $\sim 10^{-3.5}$ in the product pdf shown in Figure 7 is mainly due to these pulsars). For PSR J1711–4322 alone, the 95% upper limit for $|\Delta|$ is 5.6×10^{-4} . Since pulsars test gravitational theories in the regime of strong fields, future improvements to the above limit are important. The fact that two pulsars discovered in the last five years were able to significantly contribute to this test is encouraging and raises the possibility that additional discoveries, and improved parameters for the objects already known (particularly PSR J1711–4322 and PSR J1933–6211), will improve the limit further.

For $|\hat{\alpha}_3|$, using the updated sample of pulsars we derive a 95% upper limit of 5.5×10^{-20} . This limit is higher than the value of 4×10^{-20} derived by Stairs et al. (2005). We believe that the higher value better reflects the limits of this technique to constrain $|\hat{\alpha}_3|$ when a larger sample of pulsars is available. The most constraining pulsars for this test currently are PSR J1713+0747 and PSR J1853+1303 with very similar limits of 2.8×10^{-20} and 3.1×10^{-20} (95% confidence), respectively. The limits derived here are about 13 orders of magnitude smaller than Solar System values (Will 1993) and again test the strong field limit. Further discoveries and ongoing study of present systems (particularly PSR J1853+1303) will help to place additional constraints on this test of gravitational theories.

4. Conclusions

We have presented updated timing solutions for five MSPs, four of which are in binary systems and one which is isolated. The high precision and large time span of the observations used allowed us to measure the proper motion of these pulsars. The implied 2D space velocities in each pulsar’s standard of rest lie in the range $70\text{--}210 \text{ km s}^{-1}$. We studied the available 2D velocities of binary and isolated MSPs and find that their velocity distributions are indistinguishable with the current data. For PSR J1910+1256 and PSR J2016+1948, we are able to measure a significant rate of change of the semimajor axis which we attribute to a geometrical change in our line of sight to the pulsars due to their high space velocities. We are then able to put initial constraints on the mass of these

pulsars of $1.6 \pm 0.6 M_{\odot}$ and $1.0 \pm 0.5 M_{\odot}$ for PSR J1910+1256 and PSR J2016+1948, respectively. For PSR J1853+1303 we measured a marginal rate of change of the semimajor axis, resulting in an estimate for the pulsar mass of $1.4 \pm 0.7 M_{\odot}$.

We are also able to place updated constraints on violations of the SEP and Lorentz invariance/momentum conservation using an updated list of binary pulsars in wide orbits with small eccentricities. Using a total of 27 pulsars we derive an upper limit for the SEP violation parameter $|\Delta|$ of 4.6×10^{-3} (95% confidence) and an upper limits for the Lorentz invariance/momentum conservation violation parameter $|\hat{\alpha}_3|$ of 5.5×10^{-20} (95% confidence). Further discoveries and ongoing study of present systems will help to improve these limits.

The Arecibo Observatory, a facility of the National Astronomy and Ionosphere Center, is operated by Cornell University under a cooperative agreement with the National Science Foundation. The Parkes Radio Telescope is part of the Australia Telescope, which is funded by the Commonwealth of Australia for operation as a National Facility managed by CSIRO. We would like to thank the many collaborators who have helped with this project over the years, including D. Backer, D. Lorimer, M. McLaughlin and A. Lommen. D.J.N. was supported by NSF grant AST 0647820 to Bryn Mawr College. M.E.G. was partly funded by an NSERC PDF award. I.H.S. held an NSERC UFA during part of this work, and also acknowledges sabbatical support from the ATNF Distinguished Visitor program and from the Swinburne University of Technology Visiting Distinguished Researcher Scheme. Pulsar research at UBC is supported by an NSERC Discovery Grant.

REFERENCES

- Alpar, M. A., Cheng, A. F., Ruderman, M. A., & Shaham, J. 1982, *Nature*, 300, 728
- Archibald, A. M., et al. 2009, *Science*, 324, 1411
- Arzoumanian, Z., Joshi, K., Rasio, F., & Thorsett, S. E. 1996, in *Pulsars: Problems and Progress*, IAU Colloquium 160, ed. S. Johnston, M. A. Walker, & M. Bailes (San Francisco: Astronomical Society of the Pacific), 525
- Arzoumanian, Z., Nice, D. J., Taylor, J. H., & Thorsett, S. E. 1994, *ApJ*, 422, 671
- Avni, Y. 1976, *ApJ*, 210, 642
- Bell, J. F., & Damour, T. 1996, *Class. Quant Grav.*, 13, 3121
- Boriakoff, V., Buccheri, R., & Fauci, F. 1983, *Nature*, 304, 417
- Cadwell, B. J. 1997, Ph.D. thesis, Pennsylvania State University
- Camilo, F., Nice, D. J., Shrauner, J. A., & Taylor, J. H. 1996, *ApJ*, 469, 819
- Champion, D. J., et al. 2005, *MNRAS*, 363, 929
- Chatterjee, S., et al. 2009, *ApJ*, 698, 250
- Cordes, J. M., & Lazio, T. J. W. 2002, arXiv:astro-ph/0207156
- Cordes, J. M., & Lazio, T. J. W. 2003, arXiv:astro-ph/0301598
- Damour, T., & Esposito-Farèse, G. 1992, *Class. Quant Grav.*, 9, 2093
- Damour, T., & Schäfer, G. 1991, *Phys. Rev. Lett.*, 66, 2549
- Dehnen, W., & Binney, J. J. 1998, *MNRAS*, 298, 387
- Demorest, P., et al. 2011, *ApJ*, in preparation
- Demorest, P., et al. 2009, in *Astro2010: The Astronomy and Astrophysics Decadal Survey*, Vol. 2010, 64 (arXiv:0902.2968)
- Demorest, P. B. 2007, Ph.D. thesis, University of California, Berkeley
- Deneva, J. S., et al. 2011, *ApJ*, in preparation
- Doroshenko, O., et al. 2001, *A&A*, 379, 579
- Dowd, A., Sisk, W., & Hagen, J. 2000, in *Pulsar Astronomy - 2000 and Beyond*, IAU Colloquium 177, ed. M. Kramer, N. Wex, & R. Wielebinski (San Francisco: Astronomical Society of the Pacific), 275
- Edwards, R. T., & Bailes, M. 2001, *ApJ*, 547, L37
- Eisenhauer, F., et al. 2003, *ApJ*, 597, L121

- Foster, R. S., Cadwell, B. J., Wolszczan, A., & Anderson, S. B. 1995, *ApJ*, 454, 826
- Foster, R. S., Wolszczan, A., & Camilo, F. 1993, *ApJ*, 410, L91
- Freire, P. C. C., et al. 2011, *MNRAS*, 412, 2763
- Hobbs, G., et al. 2010, *Classical and Quantum Gravity*, 27, 084013
- Hobbs, G., et al. 2004, *MNRAS*, 352, 1439
- Hobbs, G., Lorimer, D. R., Lyne, A. G., & Kramer, M. 2005, *MNRAS*, 360, 974
- Hotan, A. W., Bailes, M., & Ord, S. M. 2006, *MNRAS*, 369, 1502
- Jacoby, B. A., et al. 2007, *ApJ*, 656, 408
- Janssen, G. H., et al. 2010, *A&A*, 514, A74
- Jessner, A., et al. 2005, *Adv. Space Res.*, 35, 1166
- Johnston, S., et al. 1993, *Nature*, 361, 613
- Kopeikin, S. M. 1996, *ApJ*, 467, L93
- Kramer, M., Wex, N., & Wielebinski, R., ed. 2000, *Pulsar Astronomy - 2000 and Beyond*, IAU Colloquium 177 (San Francisco: Astronomical Society of the Pacific)
- Kusenko, A., & Segrè, G. 1999, *Phys. Rev. D*, 59, 061302
- Löhmer, O., Lewandowski, W., Wolszczan, A., & Wielebinski, R. 2005, *ApJ*, 621, 388
- Lange, C., et al. 2001, *MNRAS*, 326, 274
- Lewandowski, W., et al. 2004, *ApJ*, 600, 905
- Lommen, A. N., et al. 2006, *ApJ*, 642, 1012
- Lorimer, D. R. 2008, *Living Reviews in Relativity*, 11, 8
- Lorimer, D. R., et al. 2006, *MNRAS*, 372, 777
- Lorimer, D. R., et al. 1996, *MNRAS*, 283, 1383
- Lorimer, D. R., et al. 1995, *ApJ*, 439, 933
- Lorimer, D. R., et al. 2005, *MNRAS*, 359, 1524
- Lyne, A. G., & Lorimer, D. R. 1994, *Nature*, 369, 127
- Lyne, A. G., et al. 1998, *MNRAS*, 295, 743
- Manchester, R. N., Hobbs, G. B., Teoh, A., & Hobbs, M. 2005, *AJ*, 129, 1993
- Manchester, R. N., et al. 2001, *MNRAS*, 328, 17
- Massey, F. J. 1951, *JASA*, 46, 68
- McLaughlin, M. A., et al. 2005, in *ASP Conference Series*, Vol. 328, *Binary Radio Pulsars*, ed. F. A. Rasio & I. H. Stairs, 43
- Navarro, J., Anderson, S. B., & Freire, P. C. 2003, *ApJ*, 594, 943
- Nice, D. J., Splaver, E. M., & Stairs, I. H. 2001, *ApJ*, 549, 516
- Nice, D. J., et al. 2005, *ApJ*, 634, 1242
- Nice, D. J., & Taylor, J. H. 1995, *ApJ*, 441, 429
- Nice, D. J., Taylor, J. H., & Fruchter, A. S. 1993, *ApJ*, 402, L49
- Olling, R. P., & Merrifield, M. R. 1998, *MNRAS*, 297, 943
- Ord, S. M., Jacoby, B. A., Hotan, A. W., & Bailes, M. 2006, *MNRAS*, 371, 337
- Peters, P. C. 1964, *Phys. Rev.*, 136, 1224
- Phinney, E. S. 1992, *Phil. Trans. Roy. Soc. A*, 341, 39
- Ransom, S. M., et al. 2011, *ApJ*, 727, L16
- Rappaport, S., et al. 1995, *MNRAS*, 273, 731
- Rawley, L. A. 1986, Ph.D. thesis, Princeton University
- Rawley, L. A., Taylor, J. H., & Davis, M. M. 1988, *ApJ*, 326, 947
- Segelstein, D. J., et al. 1986, *Nature*, 322, 714
- Splaver, E. M. 2004, Ph.D. thesis, Princeton University, Princeton, N. J., U.S.A.
- Splaver, E. M., et al. 2005, *ApJ*, 620, 405
- Spruit, H., & Phinney, E. S. 1998, *Nature*, 393, 139
- Stairs, I. H. 2004, *Science*, 304, 547

- Stairs, I. H., et al. 2005, *ApJ*, 632, 1060
- Standish, E. M. 2004, *A&A*, 417, 1165
- Tauris, T. M., & Bailes, M. 1996, *A&A*, 315
- Tauris, T. M., & Savonije, G. J. 1999, *A&A*, 350, 928
- Tauris, T. M., van den Heuvel, E. P. J., & Savonije, G. J. 2000, *ApJ*, 530, L93
- Taylor, J. H. 1992, *Phil. Trans. Roy. Soc. A*, 341, 117
- Toscano, M., et al. 1999, *MNRAS*, 307, 925
- van den Heuvel, E. P. J. 1994, in *Interacting Binaries*, ed. H. Nussbaumer & A. Orr (Berlin: Springer-Verlag), 263
- van Straten, W., et al. 2001, *Nature*, 412, 158
- Verbiest, J. P. W., et al. 2009, *MNRAS*, 400, 951
- Verbiest, J. P. W., et al. 2008, *ApJ*, 679, 675
- Wex, N. 1997, *A&A*, 317, 976
- Wex, N. 2000, in *Pulsar Astronomy - 2000 and Beyond*, IAU Colloquium 177, ed. M. Kramer, N. Wex, & R. Wielebinski (San Francisco: Astronomical Society of the Pacific), 113
- Will, C. M. 1993, *Theory and Experiment in Gravitational Physics* (Cambridge: Cambridge University Press)
- Wolszczan, A., et al. 2000, *ApJ*, 528, 907

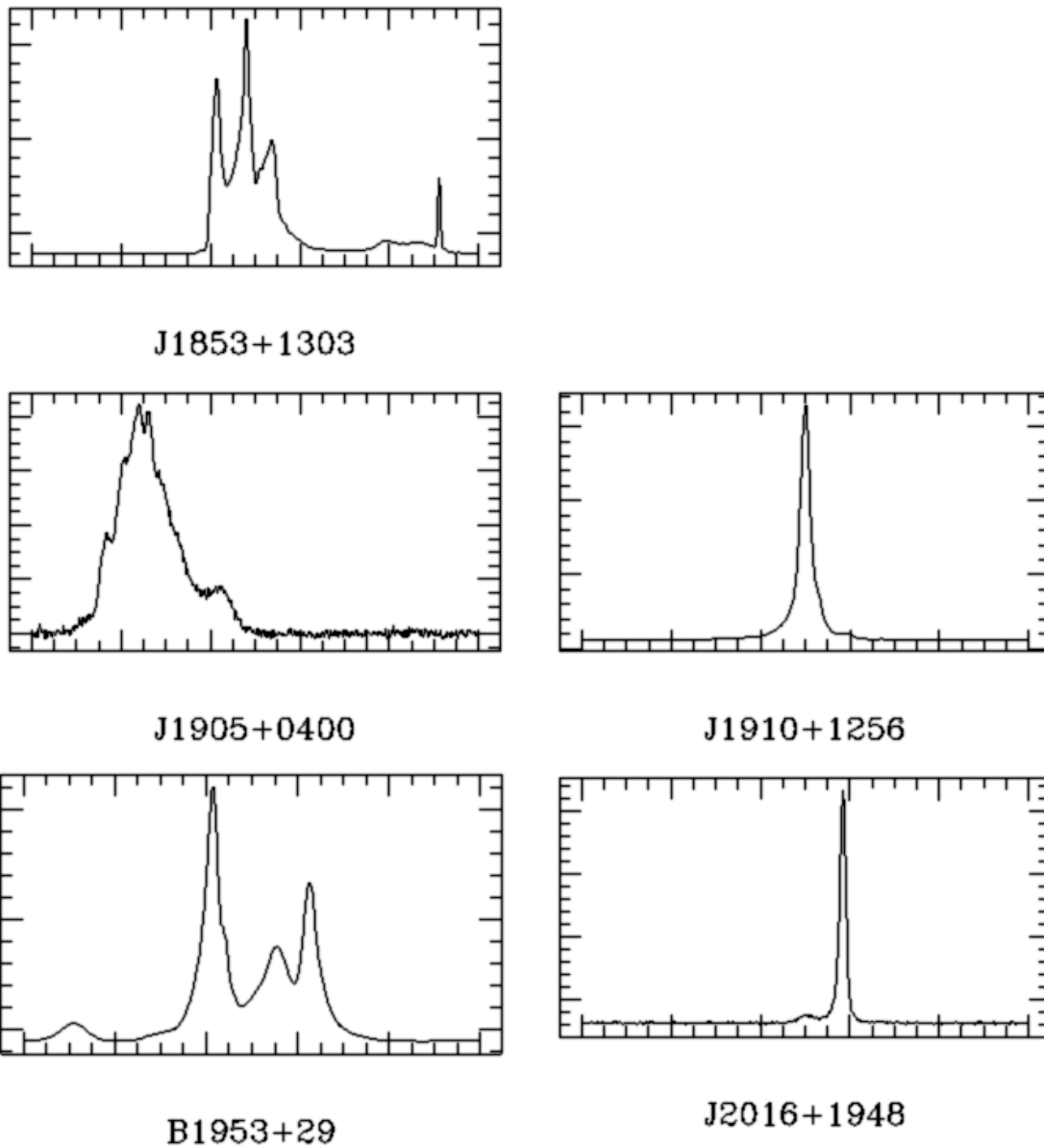


Fig. 1.— Standard profiles for each pulsar at 1400 MHz obtained by combining all the Arecibo data used in our analysis. For PSR J2016+1948 we used the WAPP data and for all other pulsars we used the ASP data. The x-axis shows one pulse period and the y-axis shows arbitrary flux units.

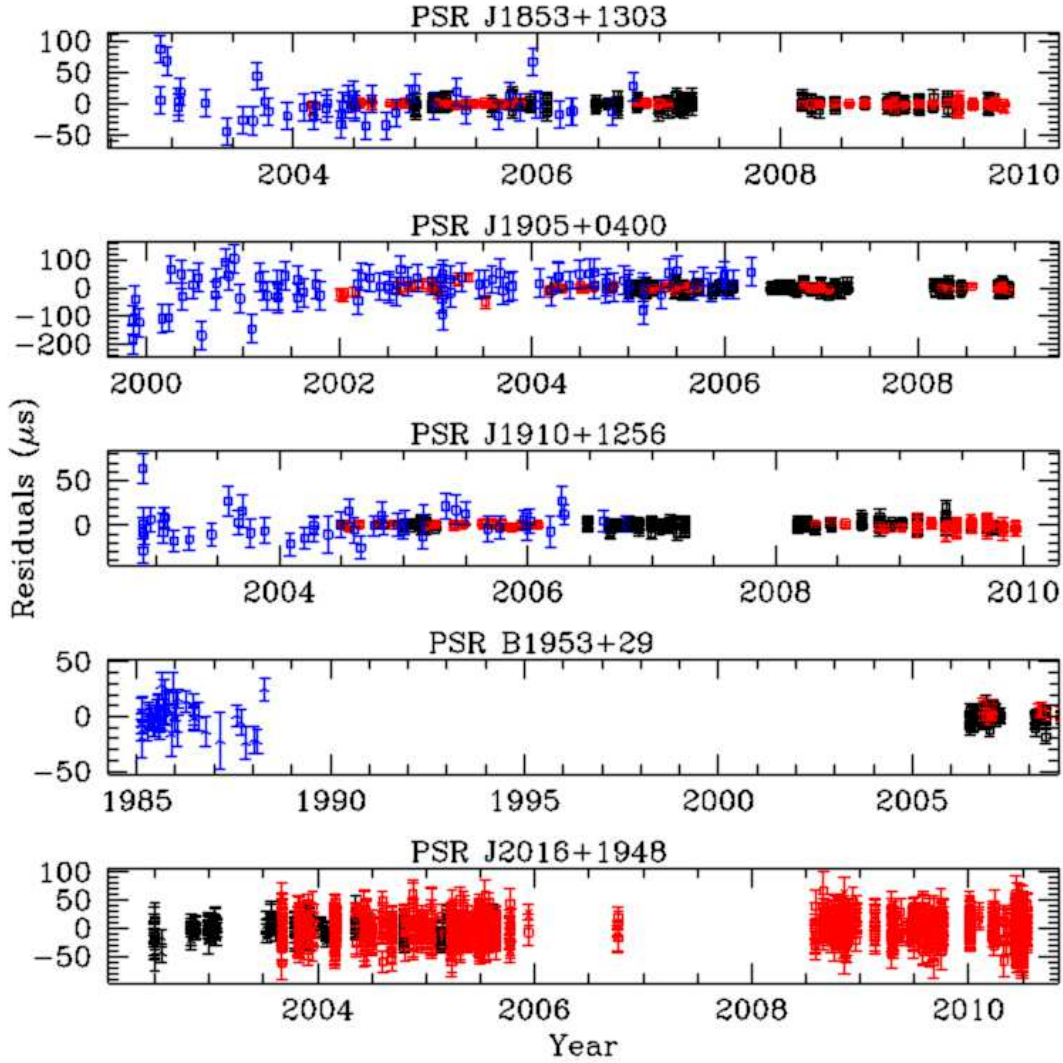


Fig. 2.— Post-fit timing residuals for each pulsar. From top to bottom we show: PSR J1853+1303, PSR J1905+0400, PSR J1910+1256, PSR B1953+29 and PSR J2016+1948. For all pulsars, the black TOAs are those obtained from ASP (except for PSR J2016+1948, where black data show the TOAs obtained with PSPM). In all cases, the red TOAs are from the WAPPs. For all pulsars, the blue TOAs are those obtained from Parkes (except for PSR B1953+29, where the blue TOAs are those from the Mark II instrument).

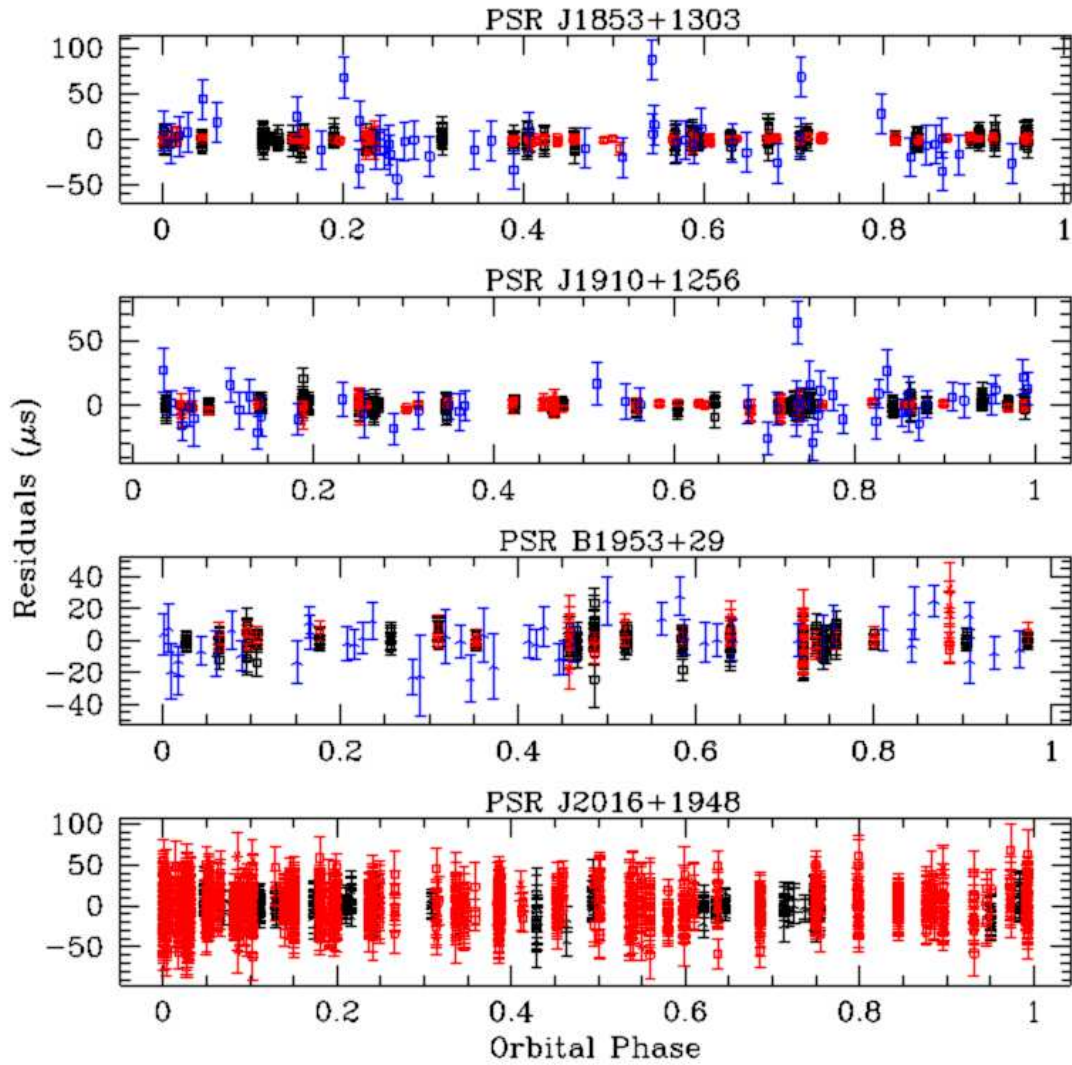


Fig. 3.— Same as for Figure 2 but showing only the binary pulsars in our sample with their residuals plotted as a function of orbital phase.

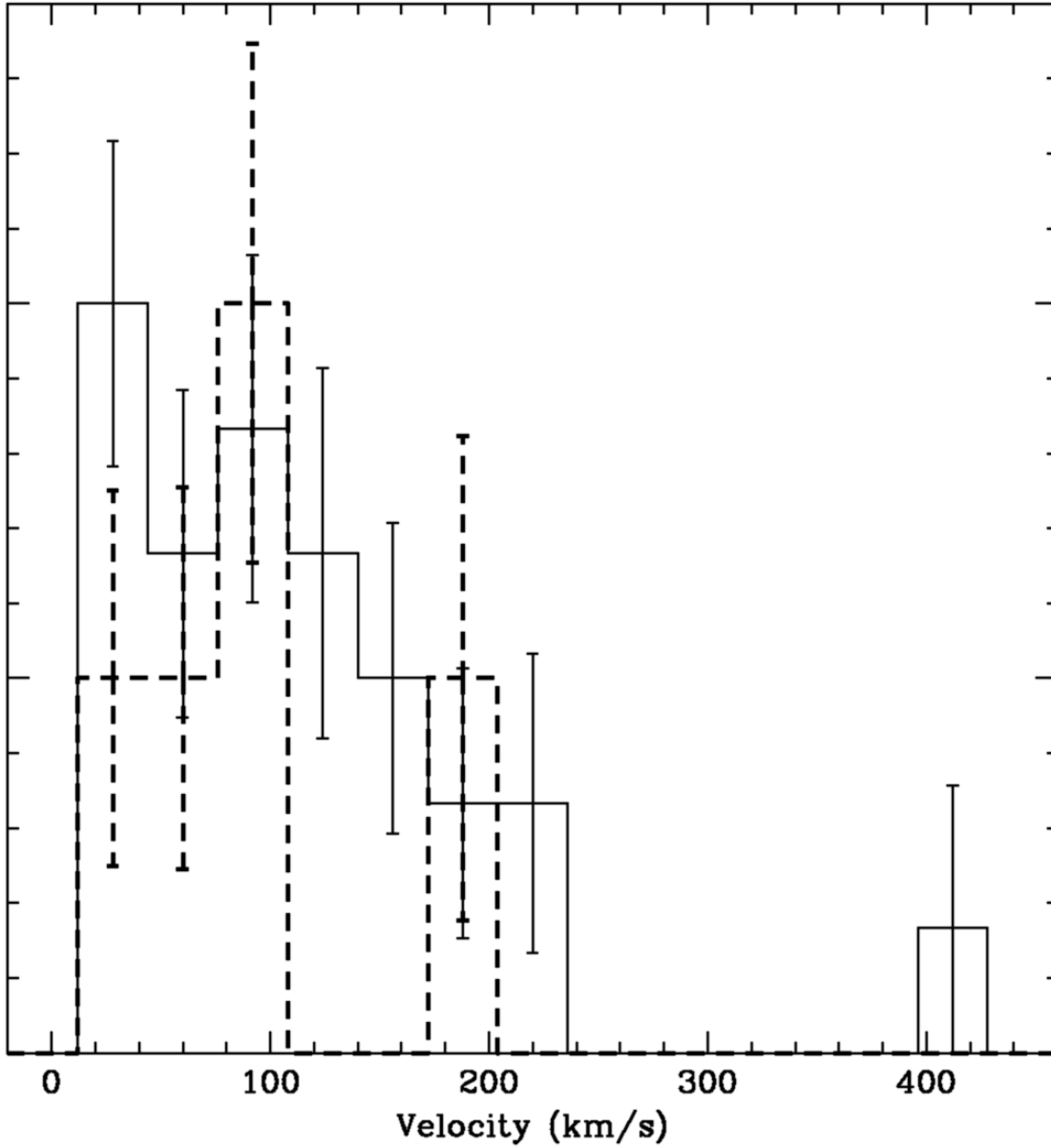


Fig. 4.— Normalized histograms of the 2D velocity distribution of binary (solid line) and isolated (dashed line) MSPs. The errors for each bin are given by the propagated measurement errors.

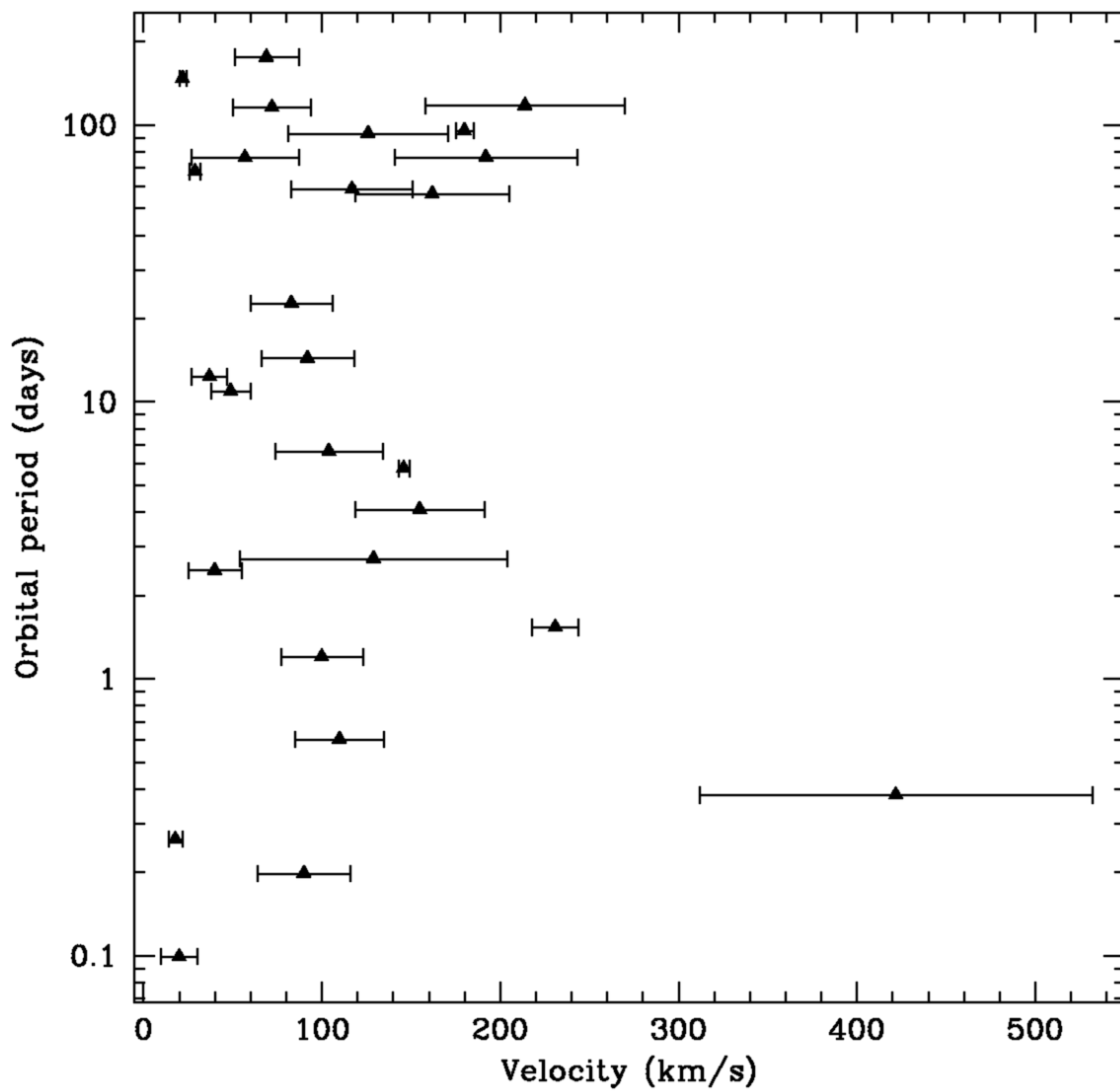


Fig. 5.— Orbital period versus 2D velocities for binary MSPs.

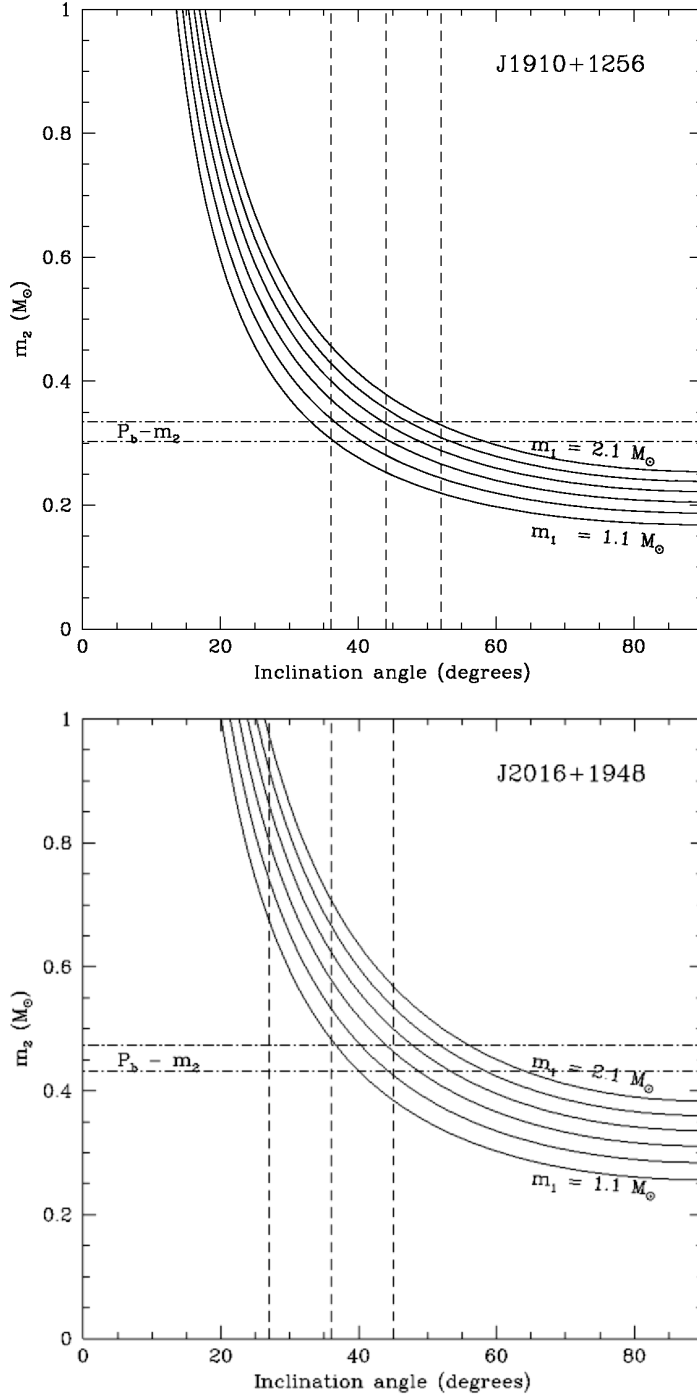


Fig. 6.— Constraints on the inclination angle, i , and companion mass, m_2 , for PSR J1910+1256 (*top*) and PSR J2016+1948 (*bottom*). Solid lines are constraints derived from the measured mass function of the systems. Vertical dashed lines represent inclination angle constraints derived from the measured \dot{x} values (centre line is the median likelihood and outer lines represent the 1σ likelihood limits). Horizontal dot-dashed lines are the m_2 values derived from the $P_b - m_2$ relationship in Tauris & Savonije (1999). See §3.2 for details.

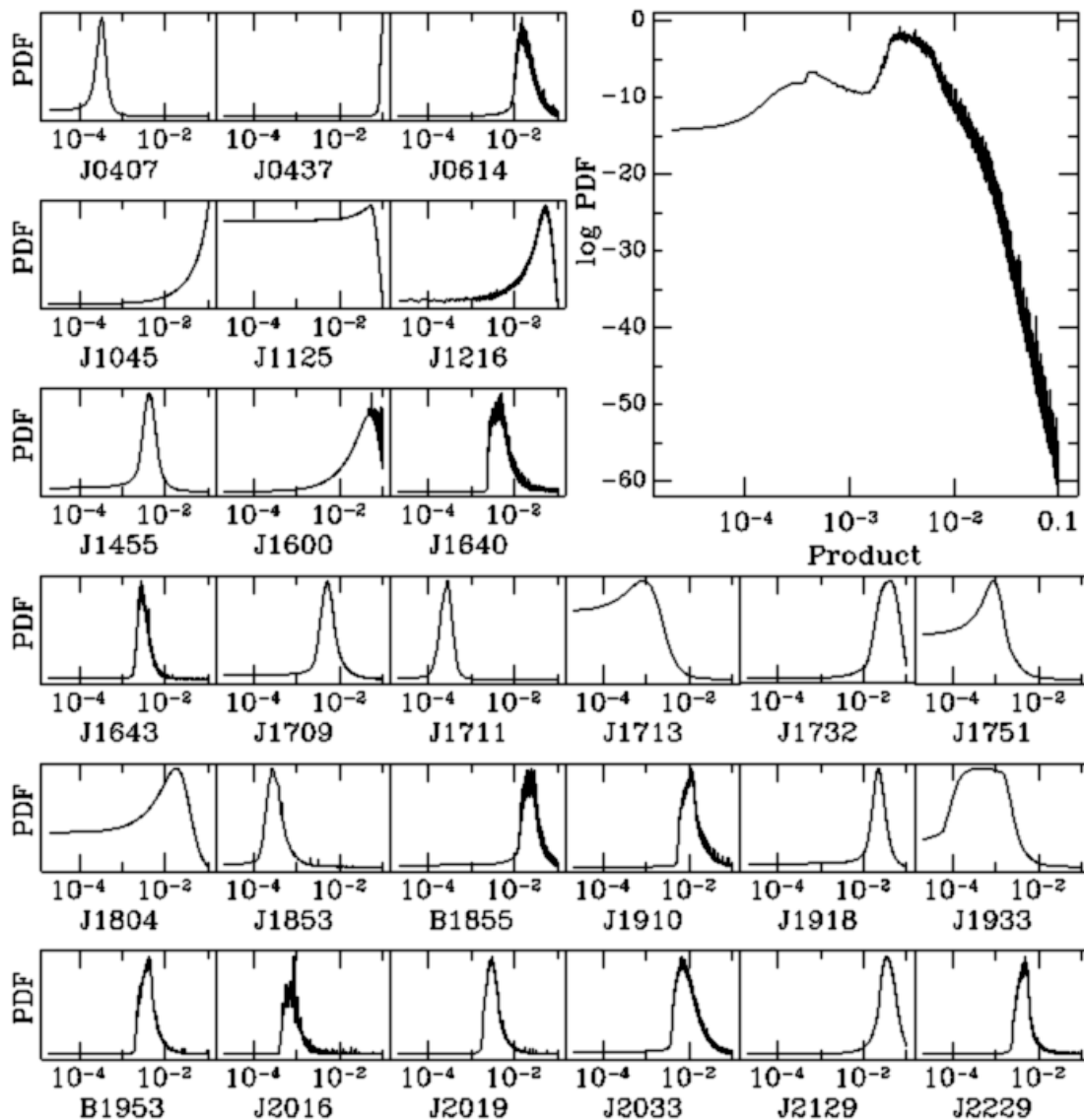


Fig. 7.— Posterior pdf's for the SEP parameter $|\Delta|$. For the individual pulsars, the y-axis is displayed on a linear scale and the x-axis on a logarithmic scale. The “product” pdf $p(|\Delta||D, I)$ in the top centre is the normalized product of the pdf's from the individual pulsars and it is shown on a log-log scale.

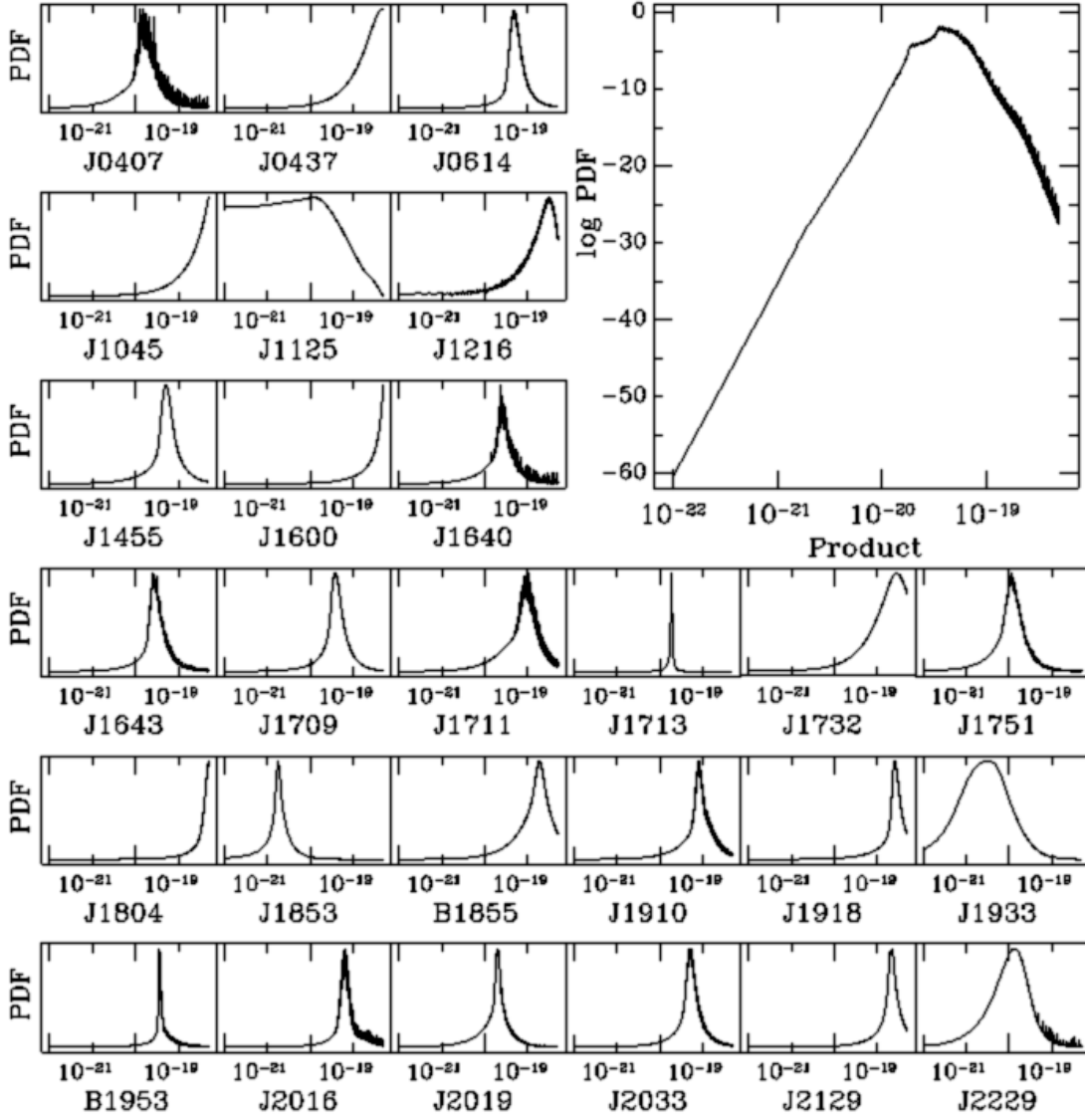


Fig. 8.— Same as Figure 7 but for the Lorentz invariance/momentum conservation parameter $|\hat{\alpha}_3|$.

Table 1: Summary of Observations

Telescope	Instrument	Number of TOAs	MJD Range	Center Frequencies (MHz)	Effective Bandwidth (MHz)
PSR J1853+1303:					
Arecibo	ASP	494	53370–55105	1400	64 or 96
	WAPP	23	54999–55105	2350	64 or 96
Parkes	Filterbank	41/32/38	53061–55134	1170/1370/1470	50/50/50
		7/8/6	54882–55134	2650/2750/2850	100/100/100
	46	52606–54023	1390	256	
PSR J1905+0400:					
Arecibo	ASP	371	53370–54808	1400	64 or 96
	WAPP	29/23/39	52279–54808	1170/1370/1470	50/50/50
Parkes	Filterbank	87	51492–53835	1390	256
PSR J1910+1256:					
Arecibo	ASP	430	53370–55105	1400	64 or 96
		49	54882–55105	2350	64 or 96
	WAPP	32/26/22	53187–55171	1170/1370/1470	50/50/50
Parkes	Filterbank	8/9/9	54882–55171	2650/2750/2850	100/100/100
		48	52602–54062	1390	256
PSR B1953+29:					
Arecibo	ASP	205	53912–55105	1400	64 or 96
	WAPP	15	54967–55106	2350	64 or 96
		17/13/13	53912–55134	1170/1370/1470	50/50/50
	Mark II	2/2/2	54882–55171	2650/2750/2850	100/100/100
47	46112–49096	430	0.96		
PSR J2016+1948:					
Arecibo	PSPM	324	52456–53591	433	7.68
	WAPP	775/355/557/199	52939–55392	1170/1310/1410/1510	100/100/100/100

Table 2: Measured and Derived Parameters for the Observed Pulsars

Parameter	PSR J1853+1303	PSR J1905+0400	PSR J1910+1256	PSR B1953+29	PSR J2016+1948
Right Ascension (RA), α (J2000.0)	18:53:57.319174(8)	19:05:28.273436(16)	19:10:09.701479(8)	19:55:27.87600(3)	20:16:57.44349(6)
Declination (Dec), δ (J2000.0)	13:03:44.0784(2)	04:00:10.8830(6)	12:56:25.5074(3)	29:08:43.4659(5)	19:47:51.5882(12)
Epoch (MJD)	54000	53700	54000	54500	53000.0
Data span (MJD)	52606.1–55134.8	51492.2–54808.8	52602.2–55171.8	46112.6–55134.9	52456.2–55392.2
Proper motion in RA, $\mu_\alpha = \dot{\alpha} \cos \delta$ (mas yr ⁻¹)	-1.68(7)	-3.80(18)	0.21(10)	-0.9(1)	1.28(26)
Proper motion in Dec, $\mu_\delta = \dot{\delta}$ (mas yr ⁻¹) ...	-2.94(12)	-7.3(4)	-7.25(12)	-4.1(1)	2.83(34)
Annual parallax, π (mas)	1.0(6)	<2.5 ^a	<0.7 ^a	<7 ^a	<4.5 ^a
Spin frequency, ν (s ⁻¹)	244.3913778653740(15)	264.242346143483(16)	200.658805375034(1)	163.04791306911(2)	15.3987376281305(13)
Spin frequency derivative, $\dot{\nu}$ (s ⁻²)	-5.2060(5) × 10 ⁻¹⁶	-3.425(1) × 10 ⁻¹⁶	-3.900(2) × 10 ⁻¹⁶	-7.901(3) × 10 ⁻¹⁶	-9.4997(14) × 10 ⁻¹⁷
Dispersion measure, DM (pc cm ⁻³)	30.5701(6)	25.6923(12)	38.0701(8)	104.501(3)	33.8148(16)
First DM derivative, \dot{DM} (pc cm ⁻³ yr ⁻¹) ...	< 4 × 10 ⁻⁴ ^a	-1.1(7) × 10 ⁻³	< 6 × 10 ⁻⁴ ^a	-4.7(2.5) × 10 ^{-3b}	-1.35(12) × 10 ^{-3b}
Orbital period, P_b (days)	115.65378643(2)		58.466742029(12)	117.34909728(4)	635.02377864(7)
Project semimajor axis, x (lt-s)	40.7695198(3)		21.1291036(3)	31.4126903(8)	150.773037(2)
Rate of change of x , \dot{x} (ls-s s ⁻¹)	1.7(7) × 10 ⁻¹⁴		-1.8(5) × 10 ⁻¹⁴	<4 × 10 ⁻¹⁴ ^a	8.3(14) × 10 ⁻¹⁴
Eccentricity, e	2.3691(12) × 10 ⁻⁵		2.3018(3) × 10 ⁻⁴	3.3025(5) × 10 ⁻⁴	1.47981(2) × 10 ⁻³
Longitude of periastron, ω (deg)	346.60(4)		106.014(9)	29.485(8)	95.6398(7)
Epoch of periastron, T_0 (MJD)	54046.78(1)		54079.318(1)	54444.267(2)	52818.648(1)
Number of TOAs	695	549	633	316	2210
Weighted rms residual (μ sec)	1.5	5.4	1.8	3.8	11.5
Derived Parameters					
Spin period, P (ms)	4.09179744490025(2)	3.78440484691321(7)	4.9835840178364(1)	6.1331666053350(1)	64.940389248427(5)
Spin period derivative, \dot{P} (s s ⁻¹)	8.7163(8) × 10 ⁻²¹	4.905(2) × 10 ⁻²¹	9.687(4) × 10 ⁻²¹	2.9734(1) × 10 ⁻²⁰	4.0063(6) × 10 ⁻¹⁹
Surface magnetic field, B (G)	1.9 × 10 ⁸	1.4 × 10 ⁸	2.2 × 10 ⁸	4.3 × 10 ⁸	5.2 × 10 ⁹
Spindown luminosity, \dot{E} (10 ³³ ergs s ⁻¹)	5.1	3.5	3.1	5.1	5.8
DM-derived distance, d_{DM} (kpc)	2.1	1.7	2.3	4.64	2.5
Characteristic age, τ_c (Gyr)	7.4	12.2	8.1	3.3	2.6
Mass function, f_1 (M_\odot)	0.00543963576(7)		0.002962840(12)	0.00241678837(2)	0.00912586(4)
Minimum companion mass ^c , m_2 (M_\odot)	0.24		0.19	0.18	0.29
Total proper motion, μ (mas yr ⁻¹)	3.39(11)	8.24(36)	6.98(14)	4.2(1)	3.11(32)
Galactic angle of proper motion ^d , Θ_μ	274°	270°	210°	197°	277°

Note— Values in parentheses are uncertainties in the last digits shown, which are twice the formal errors quoted by TEMPO after scaling the TOA uncertainties to obtain $\chi^2_\nu \simeq 1$. Right ascension values are in hours, minutes, and seconds and declination in degrees, arcminutes, and arcseconds. For all pulsars, the DE405 ephemeris was used and the recorded observatory times were corrected to TT(BIPM).

^a Value shown represents a $\Delta\chi^2 \sim 6.6$ from best fit, representing a $\sim 3\sigma$ limit (Avni 1976).

^b For PSR J2016+1948, a second DM derivative (\dot{DM}) was also measured with a value of $3.8(1.4) \times 10^{-4}$ pc cm⁻³ yr⁻². A less significant value for \dot{DM} was also measured for PSR B1953+29 giving $-2.1(1.6) \times 10^{-4}$ pc cm⁻³ yr⁻².

^c Assuming a pulsar mass of $m_1 = 1.35M_\odot$.

^d Clockwise from Galactic North.

Table 3: Proper Motions and Space Velocities of Millisecond Pulsars

Pulsar	μ_α (mas yr ⁻¹)	μ_δ (mas yr ⁻¹)	Distance (pc)	P_b (days)	V_{2D} (km s ⁻¹)	Ref.
Isolated MSPs						
J0030+0451	-5.5±0.9	< -11	310 ^a	...	<20	1
J0711-6830	-15.55±0.08	14.23±0.07	860	...	192±48	2
J1024-0719	-34.9±0.4	-47±1	200	...	48±13	3
J1730-2304	20.27±0.06	...	510	...	52±13	4
J1744-1134	18.804±0.015	-9.40±0.06	416 ^a	...	37±4	2
J1905+0400	-3.80±0.18	-7.3±0.4	1700	...	89±25	This work
B1937+21	-0.46±0.02	-0.66±0.02	3580	...	107±31	5
J1944+0907	12.0±0.7	-18±3	1800	...	197±58	2
J2124-3358	-14.12±0.13	-50.34±0.25	322 ^a	...	87±35	6
J2322+2057	-17±2	-18±3	790	...	100±30	7
Binary MSPs						
J0437-4715	121.438±0.003	-71.438±0.007	157 ^a	5.741	146±3	8
J0613-0200	1.84±0.08	-10.6±0.2	1700	1.198	100±23	2
J0751+1807	-1.3±0.2	-6.0±1.8	610	0.263	18±4	9
J1012+5307	2.4±0.2	-25.2±0.2	840	0.604	110±25	10
J1023+0038	10±1	-16±2	1300	0.198	90±26	11
J1045-4509	-6.0±0.2	5.3±0.2	1940	4.083	155±36	2
J1455-3330	5±6	24±12	530	76.174	57±30	4
J1600-3053	-0.99±0.10	-6.7±0.5	2930	14.348	92±26	12
J1640+2224	1.66±0.12	-11.3±0.2	1160	175.461	69±18	13
J1643-1224	6.0±0.1	4.1±0.4	454 ^a	147.017	22±2	2
J1709+2313	-3.2±0.7	-9.7±0.9	1400	22.711	83±23	14
J1713+0747	4.917±0.004	-3.933±0.010	1050 ^a	67.825	29±3	15
J1853+1303	-1.67±0.08	-2.91±0.12	2100	115.654	72±22	This work
B1855+09	-2.899±0.013	-5.45±0.02	910	12.327	37±10	16
J1903+0327	-2.01±0.07	-5.20±0.12	6400	95.714	180±5	17
J1909-3744	-9.510±0.007	-35.859±0.019	1270 ^a	1.533	231±13	2
J1910+1256	0.21±0.10	-7.25±0.12	2300	58.467	117±34	This work
J1911-1114	-6±4	-23±13	1220	2.716	129±75	4
J1918-0642	-7.2±0.1	-5.7±0.3	1240	10.913	49±11	18
B1953+29	-0.9±0.1	-4.1±0.1	4640	117.349	214±56	This work
B1957+20	-16.0±0.5	-25.8±0.6	2490	0.382	422±110	19
J2019+2425	-9.41±0.12	-20.60±0.15	1490	76.512	192±51	20
J2033+1734	-5.94±0.17	-11.0±0.3	2000	56.308	162±43	16
J2051-0827	5.3±1	0.3±3	1040	0.099	20±10	21
J2129-5721	9.35±0.1	-9.47±0.1	1360	6.625	104±30	2
J2229+2643	1±4	-17±4	1450	93.016	126±45	22
J2317+1439	-1.7±1.5	7.4±3.1	820	2.459	40±15	23

References: (1) Lommen et al. (2006); (2) Verbiest et al. (2009); (3) Hotan et al. (2006); (4) Toscano et al. (1999); (5) Champion et al. (2005); (6) Nice & Taylor (1995); (7) Nice & Taylor (1995); (8) Verbiest et al. (2008); (9) Nice et al. (2005); (10) Lange et al. (2001); (11) Archibald et al. (2009); (12) Ord et al. (2006); (13) Löhmer et al. (2005); (14) Lewandowski et al. (2004); (15) Splaver et al. (2005); (16) Splaver (2004); (17) Freire et al. (2011); (18) Janssen et al. (2010); (19) Arzoumanian et al. (1994); (20) Nice et al. (2001); (21) Doroshenko et al. (2001); (22) Wolszczan et al. (2000); (23) Camilo et al. (1996).

^a Distance derived using parallax. See reference for values.

Table 4: WBMSPs used for SEP and Lorentz invariance/momentum conservation tests

Pulsar	P (ms)	P_b (days)	e	ω ($^\circ$)	f_1 (M_\odot)	μ_α (mas yr^{-1})	μ_δ (mas yr^{-1})	d (kpc)	Ref.
J0407+1607	25.7017	669.0704	$9.368(6)\times 10^{-4}$	291.74(2)	0.002893	1.33	1
J0437-4715	5.7574	5.7410	$1.91685(5)\times 10^{-5}$	1.22(5)	0.001243	121.438 ± 0.003	-71.438 ± 0.007	0.157	2, 3, 4
J0614-3329	3.1487	53.5846	$1.801(1)\times 10^{-4}$	15.92(4)	0.007895	1.9	5
J1045-4509	7.4742	4.0835	$2.37(7)\times 10^{-5}$	243(2)	0.001765	-6.0 ± 0.2	5.3 ± 0.2	1.94	6
J1125-6014	2.6304	8.7526	$1(13)\times 10^{-6}$	273(87)	0.008128	1.50	7
J1216-6410	3.5394	4.0367	$7(59)\times 10^{-6}$	177(1)	0.001669	1.33	7
J1455-3330	7.9872	76.1745	$1.697(3)\times 10^{-4}$	223.81(1)	0.006272	5 ± 6	24 ± 12	0.53	8, 9
J1600-3053	3.5979	14.3484	$1.7373(2)\times 10^{-4}$	181.73(1)	0.003558	-0.99 ± 0.10	-6.7 ± 0.5	2.93	10
J1640+2224	3.1633	175.4607	$7.97262(14)\times 10^{-4}$	50.7308(10)	0.005907	1.66 ± 0.12	-11.3 ± 0.2	1.16	11, 12
J1643-1224	4.6216	147.0174	$5.0579(4)\times 10^{-4}$	321.850(4)	0.000783	6.0 ± 0.1	4.1 ± 0.4	0.454	6
J1709+2313	4.6312	22.7119	$1.87(2)\times 10^{-5}$	24.3(6)	0.007438	-3.2 ± 0.7	-9.7 ± 0.9	1.4	11, 13
J1711-4322	102.6183	922.4707	$2.375(6)\times 10^{-3}$	293.75(12)	0.003434	3.84	7
J1713+0747	4.5701	67.8251	$7.49406(13)\times 10^{-5}$	176.1915(10)	0.007896	4.917 ± 0.004	-3.933 ± 0.010	1.05	14, 15
J1732-5049	5.3125	5.2630	$9.8(20)\times 10^{-6}$	287(12)	0.002449	1.41	16
J1751-2857	3.9149	110.7465	$1.283(5)\times 10^{-4}$	45.52(19)	0.003013	1.1	17
J1804-2717	9.3430	11.1287	$3.1(5)\times 10^{-5}$	160(4)	0.003347	0.78	18, 19
J1853+1303	4.0918	115.6538	$2.3686(12)\times 10^{-5}$	346.61(4)	0.005439	-1.67 ± 0.08	-2.91 ± 0.12	2.1	This work
B1855+09	5.3621	12.3272	$2.170(3)\times 10^{-5}$	276.39(4)	0.005557	-2.899 ± 0.013	-5.45 ± 0.02	0.91	20, 21
J1910+1256	4.9836	58.4667	$2.3017(3)\times 10^{-4}$	106.016(9)	0.002962	0.21 ± 0.10	-7.25 ± 0.12	2.3	This work
J1918-0642	7.6459	10.9132	$1.991(13)\times 10^{-5}$	218.6(4)	0.005249	-7.2 ± 0.1	-5.7 ± 0.3	1.24	22
J1933-6211	3.5434	12.8194	$1.3(4)\times 10^{-6}$	116(22)	0.011749	0.52	23
B1953+29	6.1332	117.3491	$3.3026(5)\times 10^{-4}$	29.489(8)	0.002417	-0.9 ± 0.1	-4.1 ± 0.1	4.64	This work
J2016+1948	64.9404	635.0238	$1.47980(2)\times 10^{-3}$	95.640(1)	0.009126	1.28 ± 0.26	2.82 ± 0.34	2.5	This work
J2019-5721	3.9345	76.5116	$1.1109(4)\times 10^{-4}$	159.03(2)	0.010687	-9.41 ± 0.12	-20.60 ± 0.15	1.49	24, 25
J2033+1734	5.9489	56.308	$1.2876(6)\times 10^{-4}$	78.23(3)	0.002776	-5.94 ± 0.17	-11.0 ± 0.3	2.0	21
J2129-5721	3.7263	6.6255	$1.21(3)\times 10^{-5}$	196.3(1.5)	0.001049	9.35 ± 0.1	-9.47 ± 0.1	1.36	6
J2229+2643	2.9778	93.0159	$2.556(2)\times 10^{-4}$	14.42(0.05)	0.000839	1 ± 4	-17 ± 4	1.45	26, 27

References: (1) Lorimer et al. (2005); (2) Johnston et al. (1993); (3) van Straten et al. (2001); (4) Verbiest et al. (2008); (5) Ransom et al. (2011); (6) Verbiest et al. (2009); (7) Lorimer et al. (2006); (8) Toscano et al. (1999); (9) Lorimer et al. (1995); (10) Ord et al. (2006); (11) Foster et al. (1995); (12) Löhmer et al. (2005); (13) Lewandowski et al. (2004); (14) Foster et al. (1993); (15) Splaver et al. (2005); (16) Edwards & Bailes (2001); (17) Stairs et al. (2005); (18) Lorimer et al. (1996); (19) Hobbs et al. (2005); (20) Segelstein et al. (1986); (21) Splaver (2004); (22) Janssen et al. (2010); (23) Jacoby et al. (2007); (24) Nice et al. (1993); (25) Nice et al. (2001); (26) Camilo et al. (1996); (27) Wolszczan et al. (2000).